Earthquakes and Structures, Vol. 2, No. 2 (2011) 171-187
DOI: http://dx.doi.org/10.12989/eas.2011.2.2.171

Scaling of design earthquake ground motions for tall buildings based on drift and input energy demands

I. Takewaki*[1] and H. Tsujimoto[2]

[1]*Department of Architecture and Architectural Engineering, Kyoto University Kyotodaigaku-Katsura, Nishikyo-ku, Kyoto 615-8540, Japan*
[2]*Nippon Steel Corp., Futtsu 293-8511, Japan*

(Received August 20, 2010, Accepted November 17, 2010)

Abstract. Rational scaling of design earthquake ground motions for tall buildings is essential for safer, risk-based design of tall buildings. This paper provides the structural designers with an insight for more rational scaling based on drift and input energy demands. Since a resonant sinusoidal motion can be an approximate critical excitation to elastic and inelastic structures under the constraint of acceleration or velocity power, a resonant sinusoidal motion with variable period and duration is used as an input wave of the near-field and far-field ground motions. This enables one to understand clearly the relation of the intensity normalization index of ground motion (maximum acceleration, maximum velocity, acceleration power, velocity power) with the response performance (peak interstory drift, total input energy). It is proved that, when the maximum ground velocity is adopted as the normalization index, the maximum interstory drift exhibits a stable property irrespective of the number of stories. It is further shown that, when the velocity power is adopted as the normalization index, the total input energy exhibits a stable property irrespective of the number of stories. It is finally concluded that the former property on peak drift can hold for the practical design response spectrum-compatible ground motions.

Keywords: scaling of ground motion; design earthquake ground motion; maximum acceleration; maximum velocity; peak drift; earthquake input energy; Arias intensity; velocity power; acceleration power; resonant motion.

1. Introduction

The adequacy of normalization of design earthquake ground motions is essential for safer, risk-based seismic design of tall buildings (FEMA 2004, ASCE 2006, Huang *et al*. 2010). The usual intensity normalization of design earthquake ground motions using the maximum acceleration and velocity may not necessarily be reasonable from the viewpoint of physical and risk-based evaluation. While some intensity normalization methods of ground motions including structural properties have been proposed (e.g. response spectrum, energy spectrum), there are quite a few treating only the ground motion parameters.

It should also be noted that, due to inherent irregularities and uncertainties of earthquake occurrence mechanisms and ground properties, it is very difficult to predict the properties of ground

* Corresponding author, Professor, E-mail: takewaki@archi.kyoto-u.ac.jp

motions, the site of occurrence and the time of occurrence within a reasonable accuracy to be allowed in the seismic resistant design practice (Drenick 1970, Takewaki 2004, 2006, Moustafa *et al*. 2010). It is therefore desirable to develop an approach using the most unfavourable ground motion (critical excitation) among the possible ones for special structural design of important structures.

The objective of this paper is to provide the structural designers with an insight for more rational scaling of design earthquake ground motions based on drift and input energy demands. A sinusoidal motion, with a variable duration, resonant to the fundamental natural period of these building structures is treated as an approximate critical excitation for such structures. It has been shown that a long-duration far-field ground motion can be a critical excitation for high-rise buildings with longer natural periods and a near-field ground motion can be that for low-rise buildings with shorter natural periods (Tsujimoto *et al*. 2008). It is shown here that, as far as the resonant sinusoidal ground motions are concerned and the usual relation is used between the fundamental natural period of buildings and the number of stories, the maximum elastic interstory drift is directly related with the maximum velocity of the sinusoidal ground motion irrespective of the number of stories and the total input energy to structures in the elastic range is directly related with the velocity power of the input motion irrespective of the number of stories. Because the maximum deformation and the maximum input (or dissipation) energy are two major performance indices in the performance-based structural design practice, these properties appear to be very useful in constructing intensity normalization measures of ground motions. It is further shown that the former relationship holds even in the case under spectrum-compatible ground motions.

It is discussed in the last part that these relationships may hold approximately even in the inelastic range.

2. Input ground motion

2.1 Acceleration and velocity powers of sinusoidal motion

The acceleration and velocity powers (Drenick 1970, Takewaki 2004, 2006, Tsujimoto *et al*. 2008, Arias 1970, Housner and Jennings 1975) of a ground acceleration $\ddot{u}_g(t)$ are defined by

$$\int_{-\infty}^{\infty} \ddot{u}_g(t)^2 dt = \overline{C}_A \tag{1a}$$

$$\int_{-\infty}^{\infty} \dot{u}_g(t)^2 dt = \overline{C}_V \tag{1b}$$

It is known that the resonant sinusoidal motion can be an approximate critical excitation to elastic and inelastic structures under the constraint of acceleration power or velocity power (Drenick 1970, Takewaki 2004, 2006, Tsujimoto *et al*. 2008). Therefore, a resonant sinusoidal motion will be used here as the first class of input motions.

Let $\ddot{u}_g(t) = a_{\max} \sin\omega_G t$ denote the acceleration of ground motion where $a_{\max}$ and ω_G are the maximum ground acceleration and the circular frequency of the sinusoidal ground motion. The duration and natural period of the ground motion are denoted by t_0 and $T_G = 2\pi/\omega_G$, respectively. When the duration of the ground motion is given by $t_0 = n \cdot T_G/4\,(n = 1, 2,...)$, the acceleration power and velocity power can be expressed by

$$\overline{C}_A = \int_0^{t_0} \ddot{u}_g(t)^2 dt = \frac{a_{\max}^{\ 2}}{2} t_0 \tag{2a}$$

$$\overline{C}_V = \int_0^{t_0} \dot{u}_g(t)^2 dt = \frac{v_{\max}^{\ 2}}{2} t_0 \tag{2b}$$

where $v_{\max} = a_{\max}/\omega_G$ is the maximum ground velocity.

Let t_A and t_V denote arbitrary times before the ending time t_0 of input motion. The ratios $\bar{a}(t_A)$ and $\bar{v}(t_V)$ are defined by

$$\bar{a}(t_A) = \frac{\int_0^{t_A} \ddot{u}_g(t)^2 dt}{\int_0^{t_0} \ddot{u}_g(t)^2 dt} \tag{3}$$

$$\bar{v}(t_V) = \frac{\int_0^{t_V} \dot{u}_g(t)^2 dt}{\int_0^{t_0} \dot{u}_g(t)^2 dt} \tag{4}$$

The times t_{A10} and t_{A90} denote the times corresponding to $\bar{a}(t_{A10}) = 0.1$ and $\bar{a}(t_{A90}) = 0.9$, respectively, and the times t_{V10} and t_{V90} denote the times corresponding to $\bar{v}(t_{V10}) = 0.1$ and $\bar{v}(t_{V90}) = 0.9$, respectively. The effective duration of primary (intensive) ground motion is defined by the acceleration point of view ${}_et_{A0} = t_{A90} - t_{A10}$ or the velocity point of view ${}_et_{V0} = t_{V90} - t_{V10}$. An example of the effective duration ${}_et_{A0} = t_{A90} - t_{A10}$ based on the acceleration power is shown in Fig. 1.

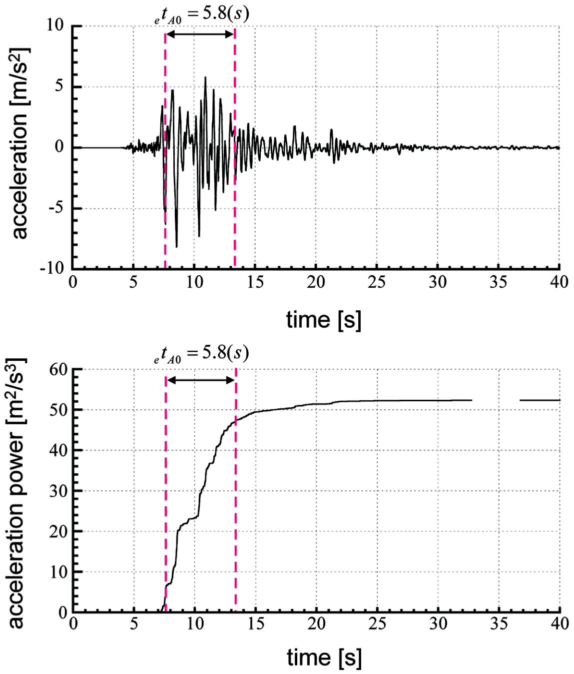

Fig. 1 Example of effective duration ${}_et_{A0} = t_{A90} - t_{A10}$ based on acceleration power

Table 1 Acceleration power, velocity power and effective duration of representative recorded ground motions

Earthquake	Site and component	C_A [m^2/s^3]	C_v [m^2/s]	${}_et_{A0}$ [s]	${}_et_{V0}$ [s]
Near fault motion/rock records					
Loma Prieta 1989	Los Gatos NS	49.5	1.49	9.1	5.9
	Los Gatos EW	19.4	0.26	6.1	5.7
Hyogoken-Nanbu 1995	JMA Kobe NS	52.4	0.79	5.8	7.9
	JMA Kobe EW	34.0	0.52	7.5	8.5
Near fault motion/soil records					
Cape Mendocino 1992	Petrolia NS	21.5	0.25	16.0	14.8
	Petrolia EW	23.9	0.51	13.9	5.6
Northridge 1994	Rinaldi NS	25.0	0.62	5.5	4.2
	Rinaldi EW	46.3	1.13	7.0	6.5
	Sylmar NS	31.3	0.86	4.4	3.9
	Sylmar EW	16.3	0.45	5.2	4.6
Imperial Valley 1979	Meloland NS	5.4	0.36	5.5	16.6
	Meloland EW	6.9	1.06	4.8	23.3
Long duration motion/rock records					
Michoacan 1985	Caleta de Campos NS	4.0	0.08	18.9	14.7
	Caleta de Campos EW	2.9	0.04	23.3	23.5
Miyagiken-oki 1978	Ofunato NS	2.4	0.01	11.8	12.1
	Ofunato EW	4.2	0.03	11.8	25.7
Long duration motion/soil records					
Chile 1985	Vina del Mar NS	34.3	0.46	41.5	43.1
	Vina del Mar EW	18.7	0.20	40.7	43.4
Olympia 1949	Seattle Army Base NS	1.3	2.29	28.0	39.6
	Seattle Army Base EW	0.9	0.02	31.8	40.3

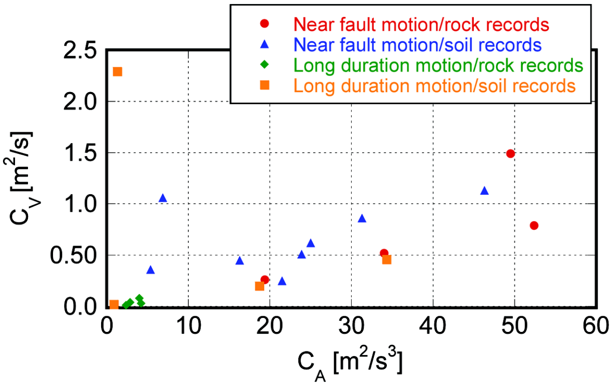

Fig. 2 Plot of velocity power versus acceleration power of four classes of recorded ground motions

The duration of the sinusoidal ground motion is determined from the natural period of the objective building structure for treating resonant cases and the data of the effective durations of actual ground motions. The near-field ground motion may be characterized by the period of 0.5s and the duration of 4s (this is critical to the 5-story building model) and the far-field ground motion may be characterized by the period of 2.0s and the duration of 36s (this is critical to the 20-story building model). The acceleration power, velocity power and the effective duration of the representative actual ground motions (Abrahamson et al., 1998) are shown in Table 1 for reference. The corresponding velocity power versus acceleration power of four classes of recorded ground motions is plotted in Fig. 2.

2.2 Pulse-like wave and long-period ground motion

Consider the second application of resonant sinusoidal ground motions. The pulse-like velocity wave is often simulated (Xu *et al*. 2007) by a modulated sinusoidal wave which is defined by

$$\dot{u}_p = Ct^n e^{-at} \sin \omega_p t \tag{5}$$

$$\ddot{u}_p = Ct^n e^{-at} [(n/t - a)\sin\omega_p t + \omega_p \cos\omega_p t] \tag{6}$$

where C, a, n and ω_p denote the amplitude scaling factor, decay factor, non-negative integer parameter controlling the skewness of the pulse envelope with respect to time and the pulse circular frequency. Fig. 3 indicates the comparison between the pulse-like velocity wave expressed by

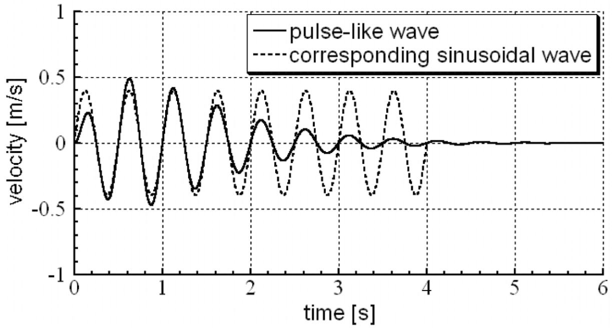

Fig. 3 Pulse-like velocity wave and sinusoidal velocity wave

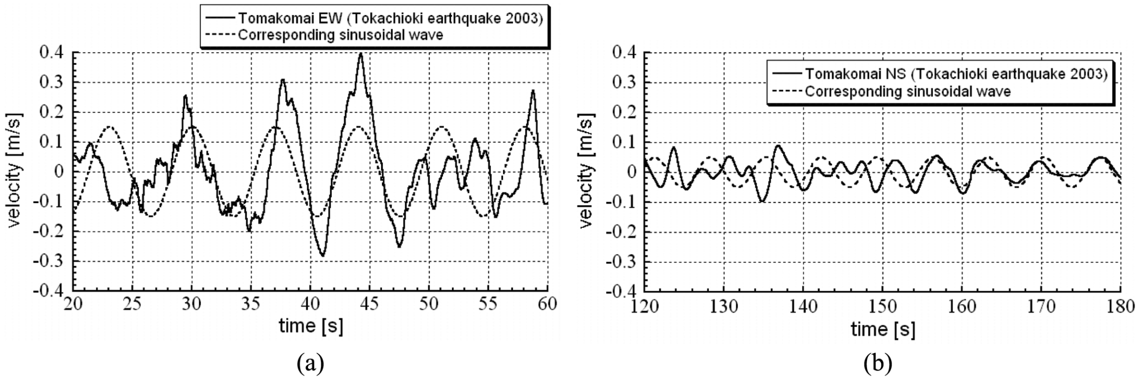

Fig. 4 Velocity waves of Tomakomai EW and NS (Tokachioki Earthquake 2003) as a representative long-period ground motion and the corresponding sinusoidal velocity wave: (a) Time interval of 20 - 60s, (b) Time interval of 120 - 180s

$T_p = 2\pi/\omega_p = 0.5$s, $n = 2$, $a = 1.5$ and $C = 2.0$ and the sinusoidal velocity wave expressed by the period of 0.5s, the duration of 4s and the maximum velocity of 0.4 m/s.

It has also been reported that there is a velocity wave similar to a sinusoidal motion in the recorded long-period ground motions and that wave could be resonant to the building structure with a long natural period. Fig. 4 shows the comparison between the Tomakomai EW and NS velocity waves (Tokachioki Earthquake of 2003) and the sinusoidal motion with the period of 7.0s.

The representation of near-field ground motions and long-period ground motions by sinusoidal waves enables one to remove uncertainties resulting from ground properties etc. and to understand clearly the response characteristics of building structures under critical inputs.

2.3 Design response spectrum by Newmark and Hall (1982)

The design spectrum-compatible ground motions can be used as the second class of input motions. A simplified version of the design displacement response spectrum by Newmark and Hall (1982) can be expressed in terms of undamped natural circular frequency ω and damping ratio h by

$$S_D(\omega;h) = S_D^A(\omega;h) = \frac{\ddot{u}_{g\max}\{3.21-0.68\ln(100h)\}}{\omega^2} = \frac{\ddot{u}_{g\max}A_A(h)}{\omega^2} \quad (\omega_U \le \omega) \tag{7a}$$

$$S_D(\omega;h) = S_D^V(\omega;h) = \frac{\dot{u}_{g\max}\{2.31-0.41\ln(100h)\}}{\omega} = \frac{\dot{u}_{g\max}A_V(h)}{\omega} \quad (\omega_L \le \omega \le \omega_U) \tag{7b}$$

$$S_D(\omega;h) = S_D^D(\omega;h) = u_{g\max}\{1.82-0.27\ln(100h)\} = u_{g\max}A_D(h) \quad (\omega \le \omega_L) \tag{7c}$$

In Eqs. 7(a) - 7(c), $u_{g\max}$, $\dot{u}_{g\max}$ and $\ddot{u}_{g\max}$ are the maximum ground displacement, maximum ground velocity and maximum ground acceleration, respectively and $A_A(h)$, $A_V(h)$ and $A_D(h)$ are the acceleration, velocity and displacement amplification factors, respectively. The circular frequencies ω_U and ω_L in Eqs. 7(a) - 7(c) are derived from the relations $S_D^A(\omega_U;h) = S_D^V(\omega_U;h)$, $S_D^V(\omega_L;h) = S_D^D(\omega_U;h)$.

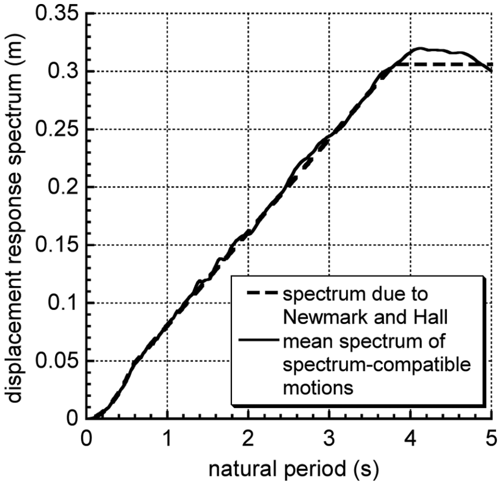

Fig. 5 Displacement response spectrum due to Newmark and Hall (1982) and mean spectrum of ten spectrum-compatible ground motions

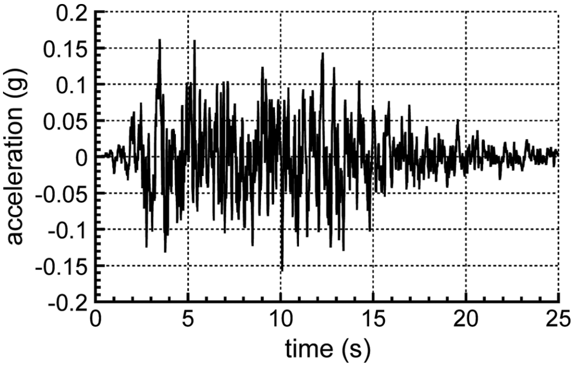

Fig. 6 Sample of acceleration of spectrum-compatible motion

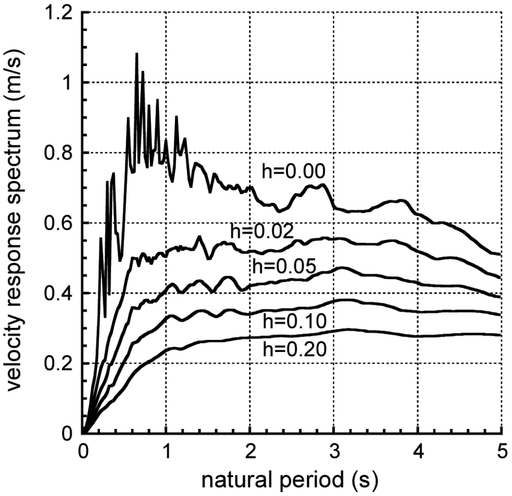

Fig. 7 Velocity response spectra for various damping ratios of a sample spectrum-compatible ground motion

Fig. 5 shows the displacement response spectrum due to Newmark and Hall (1982) and the mean spectrum of ten spectrum-compatible ground motions. Fig. 6 illustrates a sample of acceleration of spectrum-compatible motion. These spectrum-compatible ground motions are used in later sections for demonstrating the validity of the proposed relations. Fig. 7 presents the velocity response spectra for various damping ratios of a sample spectrum-compatible ground motion.

3. Building model and equivalent linear model

Consider four building structures of 5, 10, 20 and 40 stories with the same floor plan of 36 m×40 m. These building structures are modelled by shear building models as shown in Fig. 8. Assume that the present MDOF model of N stories has an equal mass m and an equal story height l in all stories and a straight-line lowest eigenmode. The assumption of the straight-line lowest eigenmode is introduced to make the formulation simple. However this restriction does not cause any difficulty in extending the present formulation to more general models. Let ω_1 denote the undamped fundamental natural circular frequency of the model. The building parameters are shown

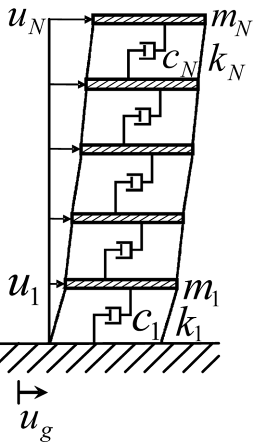

Fig. 8 Shear building model

Table 2 Parameters of main frame

Building width		6m×6 bays
Building length		8m×5 bays
Story height		3.5m
Mass / unit floor area		800 kg/m^2
Fundamental natural period T		proportional to number N of stories ($T = 0.1$ N)
Story mass	M	$m_i = 1152\times10^3$ kg
Story stiffness	k_i	determined from lowest mode of straight line
Damping coefficient	c_i	stiffness-proportional damping

in Table 2. The yield story displacement (drift) of the frame is given by 3500 mm×1/150 rad = 23 mm where 1/150 rad is the yield story deformation angle. The frame is assumed to have a normal bilinear hysteretic story shear-deformation relation as shown in Fig. 9. The ratio of the post-yield stiffness of the frame to the initial stiffness is given by 0.01 and the structural damping ratio (initial stiffness proportional one) is specified as $h_1 = 0.02$.

The response analysis is conducted by a reduced SDOF model as shown in Fig. 10(a). The equivalent mass M of the reduced SDOF model is calculated by the equivalence of the base shear in the lowest-mode vibration component.

$$\omega_1^2 m \sum_{i=1}^{N} i = \omega_1^2 M \frac{H}{l} \tag{8}$$

The equivalent height H of the mass of the reduced SDOF model is obtained from the equivalence of the overturning moment at the base in the lowest-mode vibration component.

$$\omega_1^2 m \sum_{i=1}^{N} i \cdot (il) = \omega_1^2 M \frac{H}{l} H \tag{9}$$

The equivalent mass and equivalent height can then be obtained as follows by solving Eqs. (8) and (9).

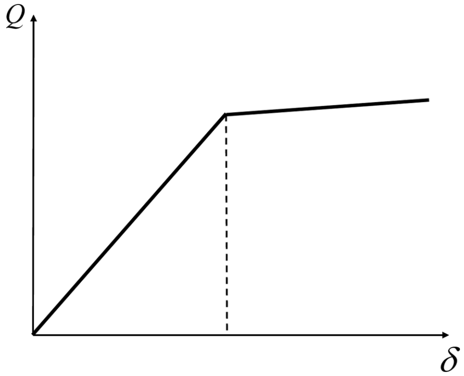

Fig. 9 Schematic diagram of relation between story shear force and drift in reduced SDOF model

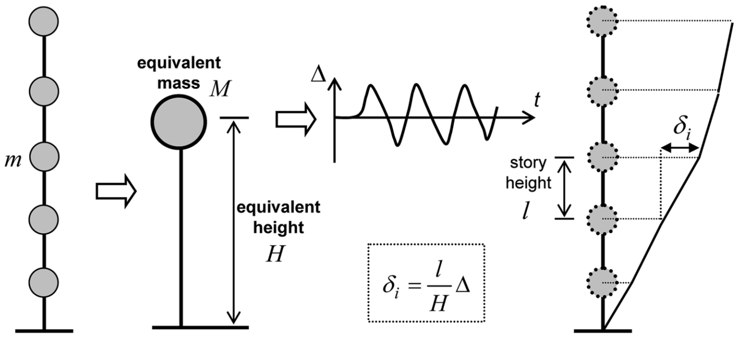

(a)

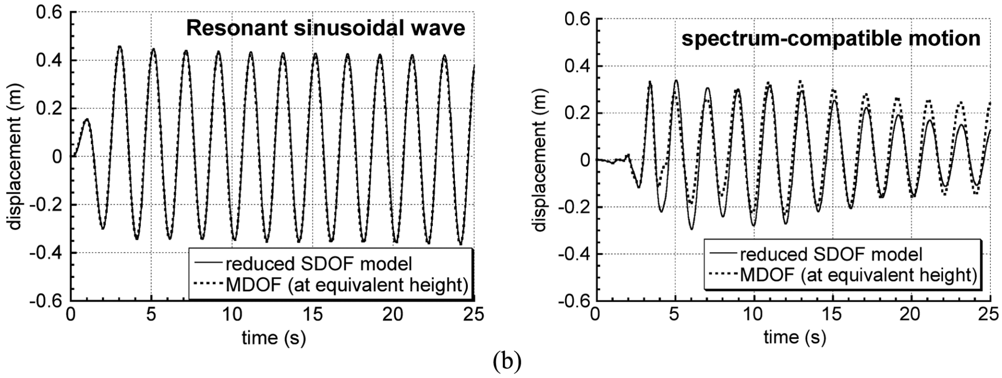

(b)

Fig. 10 Reduced SDOF model: (a) Schematic diagram for response evaluation by reduced SDOF model, (b) Accuracy of reduced SDOF model

$$M = \frac{3N(N+1)}{2(2N+1)}m \tag{10a}$$

$$H = \frac{2N+1}{3}l \tag{10b}$$

Fig. 10(b) shows the demonstration of accuracy of the SDOF model under a resonant sinusoidal motion and a spectrum-compatible motion.

In this paper, the fundamental natural period T of the building structure with the number N of stories is assumed to be expressed as $T = 0.1\,N$.

4. Scaling of ground motion based on drift and input energy demands

4.1 Relationship of the maximum interstory drift with the maximum velocity of the resonant sinusoidal ground motion

Let us consider the following resonant sinusoidal ground motion.

$$\ddot{u}_g(t) = a_{\max}\sin\omega_G t \tag{11a}$$

$$\dot{u}_g(t) = -v_{\max}\cos\omega_G t \tag{11b}$$

In Eqs. 11(a), 11(b), $a_{\max}$ and $v_{\max}$ denote the acceleration amplitude and velocity amplitude of the sinusoidal ground motion, respectively, and ω_G indicates the circular frequency of that ground motion. In this case the equations of motion for a multi-degree-of-freedom shear building model may be expressed by

$$\mathbf{M}\ddot{\mathbf{u}} + \mathbf{C}\dot{\mathbf{u}} + \mathbf{K}\mathbf{u} = -\mathbf{M}\mathbf{1}a_{\max}\sin\omega_G t \tag{12}$$

Because the proportional structural damping is assumed, the response of the s-th normal coordinate system (ω_s: s-th natural circular frequency, h_s: s-th damping ratio) can be described as

$$\ddot{q}_{0s}(t) + 2h_s\omega_s\dot{q}_{0s}(t) + \omega_s^2 q_{0s}(t) = -a_{\max}\sin\omega_G t \tag{13}$$

Consider the resonant case which is expressed by

$$\omega_1 = \omega_G \tag{14}$$

If the damping ratio is small, the first normal coordinate can be expressed as

$$q_{01} \cong (q_{01st})_0\frac{1}{2h_1}(e^{-h_1\omega_G t} - 1)\cos\omega_G t \tag{15}$$

$$(q_{01st})_0 = -a_{\max}/\omega_G^2 \tag{16}$$

Assume that the higher-order components can be neglected in the resonant situation with the first natural vibration. This has been confirmed by numerical analyses. Then the response may be described by

$$\mathbf{u} \cong \mathbf{u}_1\gamma_1 q_{01} \cong \mathbf{u}_1\gamma_1(q_{01st})_0\frac{1}{2h_1}(e^{-h_1\omega_G t} - 1)\cos\omega_G t \tag{17}$$

where γ_1 is the lowest-mode participation factor. As a normalization condition of the lowest eigenmode, put the first component of $\mathbf{u}_1$ as unity. If we take the limit $t \to \infty$, the maximum interstory drift can be reduced to

$$\delta_{j\max} \cong -\frac{1}{2h_1}\gamma_1(q_{01st})_0 \tag{18}$$

The straight-line lowest eigemode with the above-mentioned normalization condition (the first component of $\mathbf{u}_1$ is unity) leads to the following lowest-mode participation factor γ_1.

$$\gamma_1 = \frac{3}{2N+1} \tag{19}$$

Substitution of Eqs. (16) and (19) into Eq. (18) with the help of $a_{\max} = v_{\max}\omega_G$ provides

$$\delta_{j\max} \cong \frac{3}{2N+1}\frac{a_{\max}}{\omega_G{}^2}\frac{1}{2h_1} = \frac{3}{2N+1}\frac{v_{\max}}{\omega_G}\frac{1}{2h_1} \tag{20}$$

Consider only the buildings such that the fundamental natural period of the shear building model is given by the relation $T_1 = 0.1\,N$ (N: number of stories). This assumption plays a key role in this paper. Then Eq. (20) can be reduced to

$$\delta_{j\max} \cong \frac{3N}{20\pi(2N+1)}\frac{1}{2h_1}v_{\max} \tag{21}$$

The number $3N/\{20\pi(2N+1)\}$ in Eq. (21) can be shown to be almost constant (see Table 3) irrespective of the number of stories. Therefore Eq. (21) implies that, if the lowest-mode damping ratio h_1 is specified, the maximum interstory drift $\delta_{j\max}$ is proportional to the maximum ground velocity $v_{\max}$ regardless of the number of stories of buildings.

4.2 Relationship of the total input energy with the velocity power of the resonant sinusoidal ground motion

Consider the same model as in Section 3. The displacement Δ of this reduced SDOF model can be described in terms of the corresponding interstory drift δ (equal in every story) as

$$\Delta = \frac{2N+1}{3}\delta \tag{22}$$

For the amplitude, $\Delta_{\max} = (2N+1)\delta_{\max}/3$ holds.

When the number n of cycles of the sinusoidal ground motion is large, the elastic strain energy just after the end of the sinusoidal input is negligible. In this case, the total input energy during n

Table 3 Relation of the coefficients $3N/\{20\pi(2N+1)\}$ and $30\pi(N+1)/\{2(2N+1)\}$ with the number of stories

N	5	10	20	40
$3N/\{20\pi(2N+1)\}$	0.0217	0.0227	0.0233	0.0236
$30\pi(N+1)/\{2(2N+1)\}$	25.69	24.67	24.12	23.84

cycles ($=t_0/0.1\,N$) is equal to the energy dissipated by the viscous damping. By using Eqs. (2) and (21), the total input energy can be expressed by

$$\begin{aligned} E \cong W_h &= (2\pi h_1 M\omega_G{}^2\Delta_{\max}{}^2)n = (2\pi h_1 \Delta_{\max}{}^2)M\left(\frac{2\pi}{0.1N}\right)^2\left(\frac{t_0}{0.1N}\right) \\ &= \frac{\pi}{2h_1}\left\{2h_1\delta_{\max}\frac{20\pi(2N+1)}{3N}\right\}^2\frac{3N(N+1)m}{2(2N+1)}\left(\frac{t_0}{0.1N}\right) \\ &= \frac{\pi}{2h_1}v_{\max}{}^2\frac{3N(N+1)\cdot m}{2(2N+1)}\left(\frac{t_0}{0.1N}\right) = \frac{30\pi(N+1)}{2h_1(2N+1)}mC_V \end{aligned} \tag{23}$$

The number $2\pi h_1 M\omega_G{}^2\Delta_{\max}{}^2$ in Eq. (23) indicates the well-known formula for the energy dissipated in the reduced SDOF model by the viscous damping in one cycle. Furthermore the number $30\pi(N+1)/\{2(2N+1)\}$ in Eq. (23) can be shown to be almost constant see Table 3) irrespective of the number of stories. Therefore Eq. (23) implies that, if the lowest-mode damping ratio h_1 is specified, the total input energy E is proportional to the velocity power C_V of ground motion regardless of the number of stories of buildings.

This fact can also be proved in the frequency domain. The displacement Δ of the reduced SDOF model is denoted by u hereafter. The total input energy per unit mass to the reduced SDOF model can be expressed in the frequency domain by

$$\begin{aligned} \frac{E}{M} &= -\int_{-\infty}^{\infty}\dot{u}\ddot{u}_g dt = -\int_{-\infty}^{\infty}\left[\frac{1}{2\pi}\int_{-\infty}^{\infty}\dot{U}e^{i\omega t}d\omega\right]\ddot{u}_g dt = -\frac{1}{2\pi}\int_{-\infty}^{\infty}\dot{U}(\int_{-\infty}^{\infty}\ddot{u}_g e^{i\omega t}dt)d\omega \\ &= -\frac{1}{2\pi}\int_{-\infty}^{\infty}\ddot{U}_g(-\omega)\dot{U}d\omega = -\frac{1}{2\pi}\int_{-\infty}^{\infty}\ddot{U}_g(-\omega)\{H_V(\omega;\Omega,h)\ddot{U}_g(\omega)\}d\omega \end{aligned} \tag{24}$$

where $H_V(\omega;\Omega,h) = -i\omega/(\Omega^2-\omega^2+2ih\Omega\omega)$ is the velocity transfer function defined by $\dot{U}(\omega) = H_V(\omega;\Omega,h)\ddot{U}_g(\omega)$ and Ω denotes the undamped natural circular frequency of the SDOF model. $\ddot{U}_g(\omega)$ is the Fourier transform of $\ddot{u}_g(t)$. By using the relations $\ddot{U}_g(-\omega) = \ddot{U}_g{}^*(\omega)$ and $\ddot{U}_g(\omega)\ddot{U}_g{}^*(\omega) = |\ddot{U}_g(\omega)|^2$, Eq. (21) can be reduced to

$$\frac{E}{M} = \frac{1}{2\pi}\int_{-\infty}^{\infty}|\ddot{U}_g(\omega)|^2\{-\mathrm{Re}[H_V(\omega;\Omega,h)]\}d\omega = \int_0^{\infty}|\ddot{U}_g(\omega)|^2\left\{-\frac{1}{\pi}\mathrm{Re}[H_V(\omega;\Omega,h)]\right\}d\omega \tag{25}$$

In Eq. (25), $\mathrm{Re}[H_V(\omega;\Omega,h)] = -2h\Omega\omega^2/[(\Omega^2-\omega^2)^2+4h^2\Omega^2\omega^2]$ and the property of $\mathrm{Re}\{H_V(\omega;\Omega,h)]$ as an even function has been used.

It is interesting to note that the long-duration sinusoidal motion corresponds to the Dirac delta function in the frequency domain with an infinite peak at the frequency ω_G of the sinusoidal ground motion. Thus substitute $\omega = \Omega = \omega_G$ in Eq. (25). By using the relation $C_A = C_V\omega_G{}^2$ (Eq.(2)) for the resonant sinusoidal motion, Eq. (25) is reduced to

$$\frac{E}{M} = \int_0^{\infty}|\ddot{U}_g(\omega)|^2\frac{1}{2h\omega_G\pi}d\omega = \frac{1}{2h\omega_G}\frac{1}{\pi}\int_0^{\infty}|\ddot{U}_g(\omega)|^2 d\omega = \frac{1}{2h\omega_G}C_A = \frac{\omega_G C_V}{2h} \tag{26}$$

Let us rewrite the lowest-mode damping ratio by h_1 in place of h. Since the mass M of the reduced SDOF model can be expressed by $M = 3N(N+1)m/\{2(2N+1)\}$ in terms of floor mass m as stated before, the total input energy to the equivalent SDOF model can be reduced to

$$E = \frac{\omega_G C_V}{2h_1}M = \frac{30\pi(N+1)}{2h_1(2N+1)}mC_V \tag{27}$$

Eq. (27) is equivalent to Eq. (23).

4.3 Relationship of maximum interstory drift of buildings with maximum velocity of ground motion (response spectrum-compatible motion)

It can be shown mathematically in the elastic range that the property similar to Eq. (21) holds also for the spectrum-compatible ground motions. When the response amplification factor in the velocity-sensitive region is denoted by $A_V(h)$ (see Eq. 7(b)) in terms of the damping ratio h and the lowest-mode vibration component only is employed, then the maximum interstory drift is obtained by

$$\delta_{i\max} \cong \frac{3}{2N+1}\left(\frac{1}{\omega_G}\right)v_{\max}A_V(h_1) = \frac{3}{2N+1}\left(\frac{0.1N}{2\pi}\right)v_{\max}A_V(h_1) = \frac{3N}{20\pi(2N+1)}v_{\max}A_V(h_1) \tag{28}$$

where s_1 is the lowest-mode damping ratio. The expression $3N/\{20\pi(2N+1)\}$ in Eq. (28) exhibits an almost constant value irrespective of the number N of stories (see Section 4.1) and this indicates clearly the one-to-one correspondence of the maximum interstory drift with the maximum ground velocity irrespective of the number of stories.

Fig. 11 shows the maximum interstory drifts of shear building models with different numbers of stories and different damping ratios with respect to maximum velocity of ground motion obtained from Eq. (28). In this figure, $A_V(0.02) = 2.0$ is used which is based on the reference (Newmark and Hall 1982). This figure indicates the physical meaning of Eq. (28).

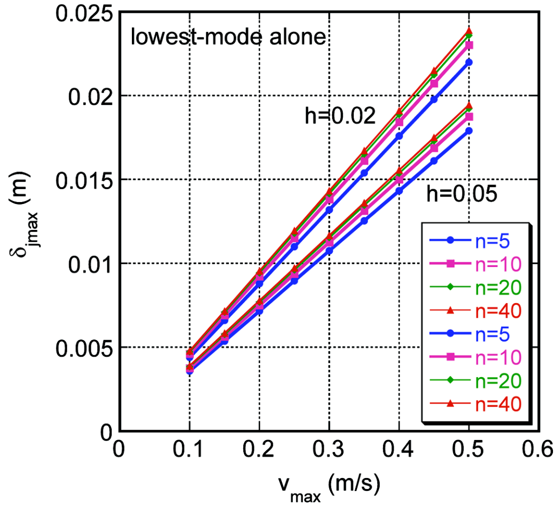

Fig. 11 Maximum interstory drifts of shear building models with different numbers of stories and different damping ratios with respect to maximum velocity of spectrum-compatible ground motion (Eq.(28))

4.4 Relationship of maximum interstory drift of inelastic buildings with maximum velocity of ground motion (resonant sinusoidal motion and response spectrum-compatible motion)

Fig. 12 shows the maximum interstory drift for the inelastic MDOF model with respect to the maximum velocity of the resonant sinusoidal ground motion. The duration of the resonant sinusoidal ground motions is 72s in this case. The interstory drift has been transformed from the response of the corresponding reduced SDOF model as in the previous sections. Furthermore Fig. 13

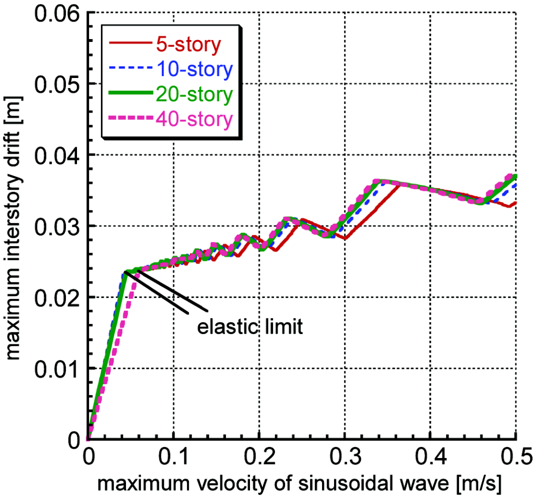

Fig. 12 Maximum interstory drift of MDOF model obtained from the corresponding inelastic SDOF system with respect to the maximum velocity of the resonant sinusoidal ground motion (post-yield stiffness ratio = 0.01, h = 0.02, original frame yield drift δ_y = 0.023 m)

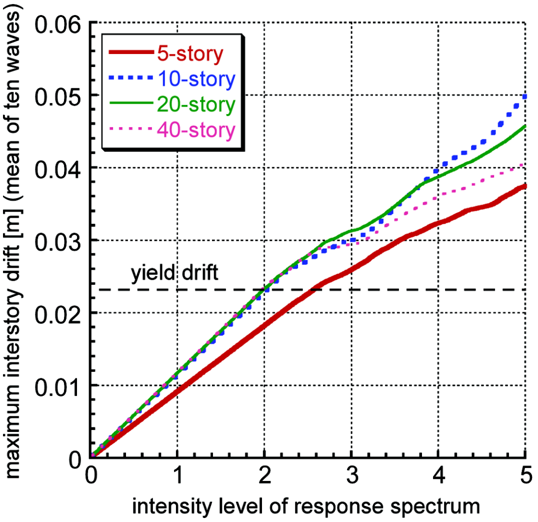

Fig. 13 Mean value of the maximum interstory drifts of MDOF model to ten spectrum-compatible motions obtained from the corresponding inelastic SDOF system with respect to the intensity level of the spectrum-compatible ground motions (post-yield stiffness ratio = 0.01, h = 0.02, original frame yield drift δ_y = 0.023 m)

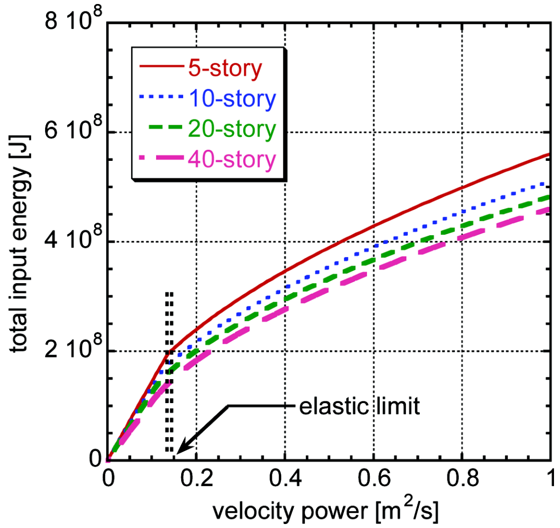

Fig. 14 Relation of total input energy with velocity power of resonant sinusoidal ground motion (post-yield stiffness ratio = 0.01, $h = 0.02$, original frame yield drift $\delta_y = 0.023$ m)

illustrates the mean value of the maximum interstory drifts to ten spectrum-compatible motions for the inelastic MDOF model with respect to the maximum velocity of the spectrum-compatible ground motions. These figures have been obtained by the time-history response analysis for the reduced SDOF model. Figs. 12 and 13 support the validity of the fact that, when the maximum ground velocity is adopted as the normalization index, the maximum interstory drift exhibits a stable property irrespective of the number of stories.

4.5 Relationship of total input energy to inelastic buildings with velocity power of resonant sinusoidal ground motion

Fig. 14 shows the relation of the total input energy under the resonant sinusoidal ground motions with the velocity power. The duration of the resonant sinusoidal ground motions is 72s in this case. This long duration is adopted by the simulation of long-period ground motions which has a strong influence on the input energy. This figure has been obtained by the time-history response analysis. It can be observed that the total input energy to elastic buildings is strongly related to the velocity power regardless of the number of stories so long as the resonant sinusoidal ground motions are concerned. This can be proved by noting that the coefficient $30\pi(N+1)/\{2(2N+1)\}$ becomes almost constant for $N \geq 5$ (see Section 4.2). Fig. 14 shows that this property can also hold approximately in the elastic-plastic buildings although the resonant property is lost in the inelastic range.

5. Conclusions

A rational scaling of design earthquake ground motions has been proposed based on drift and input energy demands. The results may be summarized as follows:

(1) Since a resonant sinusoidal motion can be an approximate critical excitation to elastic and

inelastic structures under the constraint of acceleration or velocity power, a resonant sinusoidal motion with variable period and duration has been used as an input wave of the near-field and far-field ground motions. This enables one to understand clearly the relation of the intensity normalization index of ground motion (maximum acceleration, maximum velocity, acceleration power, velocity power) with the response performance (peak interstory drift, total input energy).

(2) In order to evaluate the overall performance of building structures, it is effective to sweep out various responses (peak interstory drift, total input energy etc.) with respect to the maximum velocity or velocity power of the sinusoidal wave. This performance curve enables one to express effectively the response performance of structures to the ground motion represented by a resonant sinusoidal wave or a suite of response spectrum-compatible motions. The performance curve is useful in comparing the performances of the structures.

(3) When the fundamental natural period T of the building structure with the number N of stories is assumed to be expressed as $T = 0.1N$, the maximum ground velocity plays an important role in the performance curve of the maximum interstory drift under a resonant sinusoidal wave or a suite of response spectrum-compatible motions. More specifically, when the maximum ground velocity is adopted as the normalization index, the maximum interstory drift exhibits a stable property irrespective of the number of stories. This fact can be proved by introducing the relationship of the fundamental natural period T of the building structure with the number N of stories in the response evaluation. This property also holds approximately in the inelastic range.

(4) When the fundamental natural period T of the building structure with the number N of stories is assumed to be expressed as $T = 0.1N$, the velocity power of a resonant sinusoidal wave plays an important role in the performance curve of the total input energy. More specifically, when the velocity power is adopted as the normalization index for the resonant sinusoidal wave, the total input energy exhibits a stable property irrespective of the number of stories. This fact can be proved in the time and frequency dual domains. This property also holds approximately in the inelastic range.

Acknowledgements

This research is partly supported by the Grant-in-Aid for Scientific Research (No. 21360267). This support is gratefully acknowledged.

References

Abrahamson, N., Ashford, S., Elgamal, A., Kramer, S., Seible, F. and Somerville, P. (eds.) (1998), *Proc. of the First PEER Workshop on Characterization of Special Source Effects*, San Diego.

American Society of Civil Engineers (ASCE) (2006), *Minimum design loads for buildings and other structures,* ASCE/SEI 7-05, American Society of Civil Engineers, Reston, Virginia.

Arias, A. (1970), "A measure of earthquake intensity", In *Seismic Design for Nuclear Power Plants* (Ed. R.J. Hansen), The MIT Press, Cambridge, MA, 438-469.

Drenick, R.F. (1970), "Model-free design of aseismic structures", *J. Eng. Mech. Div. - ASCE*, **96**(EM4), 483-493.

Federal Emergency Management Agency (FEMA) (2004), *NEHRP recommended provisions for seismic regulations for new buildings and other structures*, Report No. 450-1/450-2. FEMA, Washington, D.C.

Housner, G.W. and Jennings, P. (1975), "The capacity of extreme earthquake motions to damage structures", *Structural and geotechnical mechanics*, A volume honoring N.M. Newmark edited by W.J. Hall, 102-116, Prentice-Hall Englewood Cliff, NJ.

Huang, Y.N., Whittaker, A.S. and Luco, N. (2010), "NEHRP site amplification factors and the NGA relationships", *Earthq. Spectra*, **26**(2), 583-593.

Moustafa, A., Ueno, K. and Takewaki, I. (2010), "Critical earthquake loads for SDOF inelastic structures considering evolution of seismic waves", *Earthq. Struct*., **1**(2), 147-162.

Newmark, N.M. and Hall, W.J. (1982), *Earthquake spectrum and design*, EERI., Oakland, CA.

Takewaki, I. (2004), "Bound of earthquake input energy", *J. Struct. Eng. - ASCE*, **130**(9), 1289-1297.

Takewaki, I. (2006), *Critical excitation methods in earthquake engineering*, Elsevier Science Ltd., Amsterdam.

Tsujimoto, H., Yoshitomi, S., Tsuji, M. and Takewaki, I. (2008), "Correlation of level of critical resonant sinusoidal input wave with dynamic response of building structures", *J. Constr. Steel*, **16**, 521-528. (in Japanese)

Xu, Z., Agrawal, A.K., He, W.L. and Tan, P. (2007), "Performance of passive energy dissipation systems during near-field ground motion type pulses", *Eng. Struct*., **29**, 224-236.

CC